Atmos. Chem. Phys. Discuss., 14, 18849–18877, 2014
www.atmos-chem-phys-discuss.net/14/18849/2014/
doi:10.5194/acpd-14-18849-2014

Atmospheric Chemistry and Physics Discussions

An analysis of the impacts of VOCs and NO_x on the ozone formation in Guangzhou

Y. Zou[1], X. J. Deng[1,2], B. G. Wang[2], F. Li[1], H. B. Tan[1], T. Deng[1], B. R. Mai[1], and X. T. Liu[1]

[1]Institute of Tropical and Marine Meteorology/Guangdong Provincial Key Laboratory of Regional Numerical Weather Prediction, CMA, Guangzhou, China
[2]Institute of Atmospheric Environmental Safety and Pollution Control, Jinan University, Guangzhou, China

Received: 3 June 2014 – Accepted: 21 June 2014 – Published: 17 July 2014

Correspondence to: X. J. Deng (dxj@grmc.gov.cn) and B. G. Wang (bongue@126.com)

Published by Copernicus Publications on behalf of the European Geosciences Union.

Abstract

In this study, online monitoring instruments were used to monitor ozone, NO_x and VOCs at the Guangzhou Panyu Atmospheric Composition Station (GPACS) of the China Meteorological Administration from June 2011 to May 2012, so as to obtain their characteristic seasonal and diurnal variations, as well as the impacts of NO_x and VOCs on local ozone formation and Guangzhou ozone control strategies. The results show that during the observation period the seasonal variation of ozone concentration was lower in the spring and winter and higher in the summer and autumn, which is contrary that of NO_x and VOCs. At around 09:00 LT in the summer, autumn and winter, both the ozone concentration and NO_2/NO ratio begin to increase, and the NO_2/NO ratio reached its maximum after a peak of ozone concentration, but this variation was not particularly evident in the spring. Aromatics and alkenes are the largest components for ozone formation potential, among which aromatic toluene, m-xylene, p-xylene and 1,3,5-trimethylbenzene are the most important components, with a total contribution of about 31.6 % to ozone formation potential. Through the analysis on local ozone control by the VOC/NO_X ratio, it was found that when the ozone concentration reached a peak in the summer and autumn in which high concentrations of ozone were prone to occur, ozone generation was NO_x limited, thus NO_x emissions must be controlled to regulate the occurrence of high-concentration ozone events. In the spring and winter, ozone generation was always VOCs controlled. Due to the relatively low ozone concentration, although NO_x emissions could be controlled to increase ozone concentration, high-concentration ozone events would not occur. Therefore, for the control of ozone in Guangzhou, in addition to the control of VOCs emissions, more attention must be paid to reducing NO_x emissions, so as to achieve the purpose of controlling high-concentration ozone.

ACPD
14, 18849–18877, 2014

1 Introduction

Along with its rapid economic development and urbanization, the Pearl River Delta has become one of the most serious pollution areas in China (Chan et al., 2008). Different from the air pollution situations of Beijing, Tianjin, Hebei and the Yangtze River Delta region, which involve particulate matters as the main pollutants (Wang et al., 2012; Zhao et al., 2011), due to the unique geographical location and climate as well as the rapid increase in the emissions of VOCs and NO_x ($NO + NO_2$) as ozone precursors caused by industrial activities and the growing number of motor vehicles, in the Pearl River Delta high-concentration ozone events occur frequently and are a very prominent air pollution problem (Wang et al., 2009). Tropospheric ozone is the secondary pollutant generated by photochemical reactions of VOCs and NO_x under light conditions (Sillman, 1995). However, VOCs and NO_x have no linear relationship with ozone formation, and their impacts on ozone formation can be described by VOC and NO_x control areas (Zhang et al., 2004; Tie et al., 2007; Geng et al., 2008). In 1977, Dodge used the model OZIPP (ozone isopleth plotting package) and drew an conclusion that although the specific actual situations differ, it is generally considered that when the VOC/NO_x ratio is more than 8 : 1, ozone is formed in the NO_x control area, while when the VOC/NO_x ratio is less than 8 : 1, ozone is formed in the VOCs control area (Dodge, 1977). And later this view had been adopted and applied by many researchers during their researches throughout the world (Sillman, 1999; Committee on Tropospheric Ozone Formation and Measurement, 1991; Ran et al., 2009). Therefore, the understanding of the ozone photochemical process can provide a scientific basis for the effective control of local ozone.

Currently, a greater amount of systematic long-term observation data have been available on atmospheric ozone and NO_x in the Pearl River Delta region, while VOCs data which mostly involve short-term intensive observations or non-continuous long-term observations is not included in the scope of daily observations (Wang et al., 2004; Shao et al., 2009). Therefore, the relationship between VOCs, NO_x and ozone cannot

ACPD
14, 18849–18877, 2014

be fully revealed to discern the impacts of VOCs and NO_x on ozone formation in the Pearl River Delta region. In order to more effectively solve the problem of ozone pollution in the Pearl River Delta, VOCs, NO_x and ozone were observed throughout the period of one year at GPACS, focusing on analyzing the impacts of NO/NO_2 ratio and VOCs components on ozone formation. In addition, a large amount of research has been conducted on ozone formation in the Pearl River Delta (Wang et al., 2005; Cheng et al., 2010; Guo et al., 2009). Previous studies have shown that ozone was generated in the VOCs control area of the Pearl River Delta region, but only a small number of scholars (Li et al., 2008) have analyzed the control areas of ozone formation with diurnal variation in the Pearl River Delta region. In order to control the occurrence of high-concentration ozone events in Guangzhou, the control areas of ozone formation with diurnal variation are explored in four scenarios herein, i.e. spring, summer, autumn and winter, thus providing a scientific basis for the control of ozone in Guangzhou.

This study is organized as follows. The second section describes the methodology in this study, mainly including the sampling point and observation instruments. The third section mainly analyzes the observed results, including characteristic analyses of ozone, NO_x and VOCs, the relationship between NO_2/NO ratio and ozone formation, and an analysis of the contribution of VOCs components to ozone formation by using MIR and an equivalent propylene concentration method. In the final section, the VOC/NO_x ratio analysis method is adopted to analyze the control areas with ozone formation in the seasonal diurnal variation process, in order to explore the ozone control strategies in Guangzhou.

2 Methodology

2.1 Measurements

From June 2011 to May 2012, automatic sampling and on-line monitoring were carried out on ozone, NO_x and VOCs. The sampling site was located at the moun-

ACPD
14, 18849–18877, 2014

tain top of Dazhengang, Nancun Town, Panyu District, Guangzhou City, Guangdong Province, with an elevation of 141 m, at the latitude of 23°00.236′ N and longitude of 113°21.292′ E (Fig. 1). The prevailing wind, wind speed and temperature at the sampling point during the different seasons are shown in Fig. 2 and Table 1. At the sampling point, northeasterly and southwesterly are the prevailing winds in spring (April, May and June), along with southwesterly in summer (June, July and August), southwesterly in autumn (September, October and November), and northeasterly in winter (December, January and February). In the different seasons, the average wind speed varies around1.4 m s^{-1}, while the average temperature undergoes more significant changes from 14.2 °C in winter to 29.4 °C in summer. This sampling station is a comprehensive site which is able to monitor the typical air pollution processes of the Pearl River Delta in different seasons and under different weather conditions (Deng et al., 2010).

2.2 Instrument description

The data used in this study include the hourly concentration of ozone, NO_x and VOCs during the observation period (June 2011–May 2012). The concentration of ozone gas was obtained using an EC9810B ozone analyzer produced by Ecotech Co. of Australia with the UV photometric method. The concentration of nitrogen oxides gas was collected using an EC9841B oxynitride ($NO/NO_2/NO_x$) gas analyzer produced by Ecotech with the chemiluminescence method.

VOCs concentration was obtained using a GC5000 analyzer produced by AMA Co. of Germany with the GC-FID analysis method. This apparatus is comprised of a low-boiling-point VOC analyzer and high-boiling-point BTX analyzer, including two sets of sampling systems and two systems of separated chromatographic columns. A low-boiling-point VOC analyzer was able to conduct enriched concentration at 13 °C, double adsorption at 20 °C, and desorption when the temperature was raised to 200 °C following by separation by two-dimensional chromatographic columns. The chromatographic columns comprised the Al_2O_3/Na_2SO_4 plot column with a diameter of 0.32 mm, film thickness of 5 mm and a length of 60 m, as well as a back flushing column (carbowax)

ACPD
14, 18849–18877, 2014

with a diameter of 0.32 mm, film thickness of 0.25 mm and length of 30 m. A back flushing column was used to remove the moisture component and high boiling component, and two types of chromatographic column were polar columns. Through two rounds of thermal desorption, the low-boiling-point hydrocarbons could be well separated, and the detector was a flame ionization detector (FID). A BTX high-boiling-point analyzer was able to conduct precondensation of volatile organic compounds at 30 °C, followed by thermal desorption, then separation on the DB-1 column to achieve optimum separation and prevent interference of related compounds. This column has a diameter of 0.32 mm, thickness of 10 mm and length of 60 m. A flame ionization detector (FID) was used to detect the system. The detected target compounds were 56 types of VOCs designated by the US EPA with the time resolution of once per hour. The analytical method was described in a previous study (Zou et al., 2013).

3 Results and discussion

3.1 Characteristics of ozone, NO_x and VOCs

The seasonal diurnal variation characteristics of ozone, VOCs and NO_x are shown in Fig. 3. The seasonal variation characteristics of ozone are relatively apparent. The seasonal variation of ozone concentrations display the seasonal pattern of being lower in the spring and winter and higher in the summer and autumn. Furthermore the increase range is much larger in late summer and early autumn than the other times, which is mainly due to the light, temperature and other meteorological factors being different in each season (Bloomer et al., 2009, 2010). The seasonal variation in the concentration of ozone precursors is opposite to that of ozone concentration. NO_x concentration is higher in spring and winter, but lower in summer and autumn and VOCs concentration is higher in winter, but lower in summer. The diurnal concentration variation of ozone is unimodal, reaching its maximum at 2.00 p.m., while those of the ozone precursors, i.e. VOCs and NO_x, show a bimodal variation with a peak in rush hours. These diurnal

ACPD
14, 18849–18877, 2014

concentration concentrations exhibit consistent characteristics with the law of atmospheric photochemical reactions. In order to further understand the variation in ozone concentration and reveal its dependence on photochemical reactions, it is necessary to analyze the variation trend of ozone, shown as follows:

$$d[O_3]/dt = [O_3](t + 1\,h) - [O_3](t) \quad (1)$$

In the equation, $[O_3](t)$ represents the ozone concentration at time t, and $[O_3](t + 1\,h)$ is the ozone concentration for the next hour of time t. A negative growth of variation in ozone concentration indicates that the chemical loss of ozone plays a dominant role in the variation in ozone concentration, while the contrary indicates that the generation of ozone photochemical reactions plays a key role. The results show that a negative growth of ozone concentration occurs between 15:00–23:00 LT is presumably due to titration of ozone by emissions of NO_x and the photochemical reaction do not play a key role. The zero derivative between 00:00–07:00 LT indicates no further titration with the reduction of NO_x emission. And the transmission of ozone plays an important role on keeping a relatively stable ozone concentration during the period of time. The photochemical reaction is intense at noon, and the concentration trend of ozone shows a positive growth. The photochemical generation of ozone is greater than its chemical loss (Fig. 4).

3.2 Relationship between NO_2/NO ratio and ozone formation

Atmospheric NO_2 and NO are involved in photochemical reactions, including the following:

$$O_3 + NO \rightarrow NO_2 + O_2 \quad (2)$$

$$O(3P) + O_2 + M \rightarrow O_3 + M \quad (3)$$

$$NO_2 + hv \rightarrow NO + O(3P) \quad (4)$$

These three reactions are also known as the steady-state responses, and the relationship among the three is called photo stationary state relationship. The relationship

ACPD
14, 18849–18877, 2014

between NO_2/NO and ozone in each season is shown in Fig. 5. At around 08:00 LT in the summer, autumn and winter, NO_2/NO ratio is very low due to the fact that NO is emitted from vehicle emission and the solar radiation is very weak. And the ozone concentration is also very low at this time because of titration of ozone. After that, with the strengthen of solar radiation, the ozone concentration begins to accumulate for the photolysis of NO_2 and increases with NO_2/NO ratio rising. At around 15:00 LT, the ozone concentration reaches its maximum. NO_2/NO ratio subsequently reaches its maximum by further photochemical reaction (Eq. 2). At around 19:00 LT, with the increase in NO emissions, the NO_2/NO ratio is reduced accordingly. This variation is not apparent in the spring, which may be due to meteorology in spring. However, in the actual atmosphere, the ozone concentration is also affected by VOCs, CO and other ozone precursors, and their high concentrations will in turn affect the steady-state cycle.

3.3 Impact of VOCs on ozone formation potential

VOCs appear in various types. Different types of VOCs have different photochemical reactivities, thereby leading to different ozone formation potential. Ozone control is mainly used to control the species with the largest ozone formation potential, which is the most cost-effective solution. VOCs have three main factors for ozone formation potential: carbon-number concentration (ppbc), kinetic activity, and mechanism activity. Therefore, it is necessary to analyze VOCs components through the three factors of ozone formation.

For kinetic activity, the propylene-equivalent concentration method (C_{PE} (J)) is expressed as shown below:

$$C_{PE}(J) = C_J K_{OH}(J)/K_{(OH)}(C_3H_6) \quad (5)$$

In the equation, J represents a species of VOC, C_J represents the carbon-number concentration (ppbc) of this species, and $K_{OH}(J)$ and $K_{OH}(C_3H_6)$ denote the chemical

ACPD
14, 18849–18877, 2014

reaction rate constant in the free radical reaction of species J and propylene with OH. The reaction rate constant is shown in Table 2.

For the mechanism activity, the MIR factor weighting method is used with the following expression:

$$\mathrm{Con}_{\mathrm{j.MIR}} = \mathrm{MIR} \times \mathrm{Com}_{\mathrm{ppbv}} \times u_{\mathrm{j}}/u_{\mathrm{ozone}} \quad (6)$$

In the equation, u_{j} and u_{ozone} represent the relative molecular mass of species J in the VOCs and ozone respectively, $\mathrm{Com}_{\mathrm{ppbv}}$ represents the actual volume mixing ratio, the Maximum Incremental Reactivity (MIR) factors were developed by Carter (Carter et al., 1994) in model Scenarios, MIR of each VOCs is from the model and $\mathrm{Con}_{\mathrm{j.MIR}}$ is maximum-increment-activity MIR factor weighting concentration which represents the maximum ozone concentration generated by this species based on MIR. The maximum ozone concentrations of different VOCs are used to compare their relative ozone formation potential. The MIR coefficients are shown in Table 2.

Figure 6 shows the characteristics of VOCs components obtained at the sampling point by using the volume mixing ratio concentration (ppbv), carbon number concentration (ppbc), propylene-equivalent concentration (ppbc), and maximum-increment-activity MIR factor weighting concentration (ppbv) methods. As viewed from the volume mixing ratio concentration (ppbv), hydrocarbons occupy the largest proportion, accounting for 59 % of total VOCs concentration, among which low-carbon compounds (fewer than five carbon atoms) are dominant, accounting for 41.2 %, followed by aromatics (24 %), and alkenes have the lowest proportion, at 17 %. As viewed from carbon concentration (ppbc), alkanes have the largest proportion of 53 %, the aromatic proportion rises to 36 %, and alkenes have the lowest proportion of 11 %. It is thus shown that when using the volume mixing ratio concentration, the importance of low-carbon alkane compounds will be overestimated. As viewed from the propylene-equivalent and MIR factor weighting concentrations, the alkenes and aromatics are dominant, accounting for total proportions of 73 % and 83 % respectively, and alkanes have the lowest proportion. Total propylene-equivalent concentration accounts for nearly half of

ACPD
14, 18849–18877, 2014

the total carbon concentration, indicating that the activities of major VOCs components are lower than propylene at the sampling point. In summary, during the monitoring period, as viewed from the volume mixing ratio and carbon number concentrations of VOCs, alkanes and aromatics are shown to be the most important constituents of the atmosphere at the sampling point. However, as viewed from ozone formation potential, aromatics and alkenes are the two species with the largest contributions. Alkanes content are high, but because of its low reactivity, alkanes have less contribution to the reactivity of VOCs and ozone formation potential. Although the alkenes concentration are smaller than that of alkanes, due to its high reactivity, alkenes have greater contributions to ozone than alkanes. Table 3 shows the ozone formation potential ranking of VOCs species as calculated by the propylene-equivalent concentration and MIR factor methods. It can be seen that the results of both methods are partially consistent, but some differences may also be seen. Among the top 10 species, eight species are exactly the same, differing only in terms of rank order. It is shown that both methods can be used to reflect the ozone formation potential of each VOCs species to some extent, and especially those with greater contributions to ozone formation have better consistency. However, since these two methods differ in principle, the calculated ranks of ozone formation potential are also different. The propylene-equivalent concentration method only considering kinetic activity ignores the differences in mechanism activities of the reaction between peroxide radicals and NO, thus when assessing ozone formation potential, the species with faster OH reaction rate may be overestimated, such as isoprene. Although the MIR factor method considers the kinetics and mechanism activity, due to the fact that the MIR factor involves possible uncertainty and the lack of MIR data for some species, the MIR factor method cannot become a reliable assessment approach of ozone formation potential. In summary, aromatics are the species with the highest reactivity at the sample point, followed by alkenes. Aromatics have a high carbon concentration in the ambient atmosphere with high activity, in which toluene, m-xylene, p-xylene and 1,3,5-trimethylbenzene with higher reactivity are the most important, with a total contribution to ozone formation potential of about 31.61 %. These

ACPD
14, 18849–18877, 2014

substances are mainly sourced from large factories and industrial activities (Liu et al., 2008a). As an industrial city, Dong guan is located in the eastern part of the sampling point, where EN wind is the prevailing in the autumn and winter at the sampling points. Dongguan is presumed to have some contributions to VOCs at sampling points in the autumn and winter. Moreover, isoprene has no high concentration, but ranks at no. 1 and 3 in terms of OH activity and MIR. Therefore, the choice of green plant species must consider the isoprene emissions of plants in the greening process at the sampling point.

3.4 Sensitive areas of ozone formation

As mentioned in Sect. 3.2, if only steady-state reaction occurs in the atmosphere, no net formation of ozone exists, but in the actual atmosphere, ozone formation is also affected by VOCs and other precursors.

$$OH + RH \rightarrow R + H_2O \quad (7)$$

$$R + O_2 + M \rightarrow RO_2 + M \quad (8)$$

$$RO_2 + NO \rightarrow RO + NO_2 \quad (9)$$

$$RO + O_2 \rightarrow R'CHO + HO_2 \quad (10)$$

$$HO_2 + NO \rightarrow OH + NO_2 \quad (11)$$

NO_2 produced by Eqs. (9) and (11) can generate ozone, and the radical regenerated by Eqs. (10) and (11) can excite a cycle. In the formation of the tropospheric ozone, the reaction of VOCs and NO_x with free radicals plays an important role. It can be seen that the ozone formation relies on the VOC/NO_x ratio. VOCs and NO_x have a non-linear relationship with the formation of the ozone as a secondary photochemical product, and their impacts on the ozone formation can be described by the VOCs and NO_x control areas. In 1977, Dodge used the model OZIPP (ozone isopleth plotting package) and drew an conclusion that although the specific actual situations differ, it is generally considered that when the VOC/NO_x ratio is more than 8 : 1, ozone is formed in the

ACPD
14, 18849–18877, 2014

NO_x control area, while when the VOC/NO_x ratio is less than 8 : 1, ozone is formed in the VOCs control area (Dodge, 1977). And later this view had been adopted and applied by many researchers during their researches throughout the world (Sillman, 1999; Committee on Tropospheric Ozone Formation and Measurement, 1991; Ran et al., 2009). We also use this VOCs/NO_x ratio value (8) to research the ozone formation in Guangzhou for the reason that the VOC/NO_x ratio has not yet been confirm in Guangzhou to judge whether the ozone is formed in the VOCs control area and NO_x control area.

Most previous studies in the PRD region reported that ozone was VOC-limited (Zhang et al., 2008b; Guo et al., 2009). However, few previous studies on the region's ozone formation regime have examined the possible diurnal variations in ozone formation regime. An analysis was carried out on the diurnal variation of seasonal ozone concentration and the VOC/NO_x ratio during the monitoring period (Fig. 7). It was found that high-concentration ozone events are prone to occur in the summer and autumn. In the morning (7:00 to 08:00 LT), the VOC/NO_x ratio is less than 8, and ozone is formed in the VOCs control area, leading to a decline in VOCs concentration, which helps to further reduce the ozone concentration. However, when the ozone concentration reaches a peak at noon, the VOC/NO_x ratio is greater than 8, and ozone is formed in the NO_x control area. The NO_x emissions must be controlled to achieve the purpose of controlling high-concentration ozone events, which is similar to the research findings of Pearl River Delta (Li et al., 2013). In the spring and winter, the VOC/NO_x ratio is always less than 8, and ozone is generated in the VOCs control area for a long period of time. Since the ozone concentration is relatively low in these two seasons, although the control of NO_x emissions can increase the ozone concentration, no high-concentration ozone event will occur. Therefore, for the control of the local ozone, in addition to VOCs control, the control of NO_x concentration will further reduce high ozone concentration to prevent the occurrence of high-concentration ozone events.

The high-concentration ozone is seriously harmful to human health, many regulators are focusing on reducing emissions at peak ozone forming hours (Castellanos et al.,

ACPD
14, 18849–18877, 2014

2009). In order to further study the ozone control strategies under the conditions of high-concentration ozone, the days with high-concentration ozone were selected for analysis in the monitoring period; the day with high-concentration ozone refers to the day with an hourly ozone value higher than 93 ppbv. It may be seen in Fig. 8 that under the conditions of high-concentration ozone at noon, the control of NO_x concentration may transiently reduce the peak of high-concentration ozone. However, when the ozone concentration is relatively low in the morning and at night, the control of the NO_x concentration may transiently increase the ozone concentration. Therefore, when high-concentration ozone events occur, more attention must be paid to controlling NO_x emissions, so as to achieve the purpose of controlling high-concentration ozone events.

4 Conclusions

One-year consecutive observation was carried out on the near-surface ozone and its precursors VOCs and NO_x at GPACS, and the seasonal and diurnal variations were characterized. The results indicate that seasonal variation in the ozone concentration is significantly shown as being lower in the spring and winter and higher in the summer and autumn, while the precursors VOCs and NO_x display the opposite seasonal variation against the ozone. The diurnal concentration variation of the ozone shows a unimodal variation, which reaches its maximum at 14:00 LT, while that of the ozone precursors VOCs and NO_x display a bimodal variation, which reach their maximum around rush hour. A negative growth of ozone concentration occurs between 15:00–23:00 LT is presumably due to titration of ozone by emissions of NO_x and the photochemical reaction do not play a key role. The photochemical reaction is intensive at noon, so that the variation trend of the ozone concentration shows a positive growth, and photochemical formation of the ozone is larger than its chemical loss. Through analyzing the relationship between NO_2/NO ratio and ozone concentration, it is found that at around 09:00 LT in the summer, autumn and winter, both the ozone concentration and NO_2/NO ratio begin to increase, and the NO_2/NO ratio reaches its maximum

ACPD
14, 18849–18877, 2014

after the peak of ozone concentration. In the spring, the NO_2/NO ratio performs differently from the other three seasons, which may be due to the spring weather factors. Through analyzing the impacts of the VOCs components on ozone formation, it is revealed that, as viewed from the volume mixing ratio concentration and carbon number of VOCs, alkanes and aromatics are the most important atmospheric constituents at the sampling point. As viewed from ozone formation potential, aromatics and alkenes are the two species with the largest contributions. Among these, toluene, m-xylene, p-xylene and 1,3,5-trimethylbenzene are the most important, with a total contribution to ozone formation potential of about 31.6 %. It should be noted that the concentration of isoprene emitted by plants is not high, but has a very large contribution to the ozone. Through analyzing the diurnal variation law of seasonal ozone concentration and the VOC/NO_x ratio, it is found that high-concentration ozone events are prone to occur in the summer and autumn. In the morning (07:00 to 08:00 LT), ozone is formed in the VOCs control area, and the reduction of VOCs concentration helps to further reduce the ozone concentration. However, when the ozone concentration reaches its peak at noon, the ozone is formed in the NO_x control area. The NO_x emissions must be controlled to achieve the purpose of controlling high-concentration ozone events. However, in the spring and winter, ozone is generated in the VOCs control area for a long period of time. Due to the fact that the ozone concentration is relatively low in these two seasons, although the control of the NO_x emissions can increase the ozone concentration, no high-concentration ozone event will occur. Through further analysis of the days with high-concentration ozone, it is found that when high-concentration ozone events occur, more attention must be paid to controlling NO_x emissions.

Acknowledgements. This research work is funded by the National Natural Science Foundation of China (41175117, 40875090), National "973" Program (2011CB403400), Natural Science Foundation of Guangdong Province (S2012010008749), Special Research Project of Public Service Sectors (Weather) (GYHY201306042), and Science and Technology Sponsorship Program of Guangdong Province (2010A030200012)

ACPD
14, 18849–18877, 2014

References

Atkinson, R. and Arey, J.: Atmospheric degradation of volatile organic compounds, Chem. Rev., 103, 4605–4638, 2003.

Bloomer, B. J., Stehr, J. W., Piety, C. A., Ross, J. S., and Dickerson, R. R.: Observed relationships of ozone air pollution with temperature and emissions, Geophys. Res. Lett., 36, L09803, doi:10.1029/2009GL037308, 2009.

Bloomer, B. J., Vinnikov, K. Y., and Dickerson, R. R.: Changes in seasonal and diurnal cycles of ozone and temperature in the eastern US, Atmos. Environ., 44, 1–9, 2010.

Carter, W. P. L.: Development of ozone reactivity scales for volatile organic compounds, J. Air Waste Manage., 44, 881–899, 1994.

Castellanos, P., Stehr, J. W., Dickerson R. R., and Ehrman, S. H.: The sensitivity of modeled ozone to the temporal distribution of point, area, and mobile source emissions in the eastern United States, Atmos. Environ., 43, 4603–4611, 2009.

Chan, C. K. and Yao, X. H.: Air pollution in mega cities in China, Atmos. Environ., 42, 1–42, doi:10.1016/j.atmosenv.2007.09.003, 2008.

Cheng, H. R., Guo, H., Saunders, S. M., Lam, S. H. M., Jiang, F., Wang, X. M., Simpson, I. J., Blake, D. R., Louie, P. K. K., and Wang T. J.: Assessing photochemical ozone formation in the Pearl River Delta with a photochemical trajectory model, Atmos. Environ., 44, 4199–4208, 2010.

Committee on Tropospheric Ozone Formation and Measurement: Rethinking the Ozone Problem in Urban and Regional Air Pollution, Natl. Acad. Press, Washington, DC, 1991.

Deng, X. J., Wang, X. M., Zhao, C. S., Ran, L., Li, F., Tan, H. B., Deng, T., Wu, D., and Zhou, X. J.: The mean concentration and chemical reactivity of VOCs of typical processes over Pearl River Delta Region, China, Environ. Sci., 30, 1153–1161, 2010.

Dodge, M. C.: Combined use of modeling techniques and smog chamber data to derive ozone precursor relationships, Proceedings of the international conference on photochemical oxidant pollution and its control, 2, 881–889, 1977.

Geng, F. H., Tie, X. X., Xu, J. M., Zhou, G. Q., Peng, L., Gao, W., Tang, X., and Zhao, C. S.: Characterizations of ozone, NO_x, and VOCs measured in Shanghai, China, Atmos. Environ., 42, 6873–6883, 2008.

Guo, H., Jiang, F., Cheng, H. R., Simpson, I. J., Wang, X. M., Ding, A. J., Wang, T. J., Saunders, S. M., Wang, T., Lam, S. H. M., Blake, D. R., Zhang, Y. L., and Xie, M.: Concurrent

ACPD
14, 18849–18877, 2014

observations of air pollutants at two sites in the Pearl River Delta and the implication of regional transport, Atmos. Chem. Phys., 9, 7343–7360, doi:10.5194/acp-9-7343-2009, 2009.
Li, Y.: Numerical Studies on Ozone Source Apportionment and Formation Regime and their Implications on Control Strategies, Hong Kong University of Sci. & Tech., Hong Kong, 2011.
Li, Y., Lau, K. H., Fung, C. H., Zheng, J. Y., and Liu, S. C.: Importance of NO_x control for peak ozone reduction in the Pearl River Delta region, J. Geophys. Res., 118, 9428–9443, 2013.
Liu, Y., Shao, M., Fu, L. L., Lu, S. H., Zeng, L. M., and Tang, D. G.: Source profiles of volatile organic compounds (VOCs) measured in China: part I, Atmos. Environ., 42, 6247–6260, 2008.
Ran, L., Zhao, C. S., Geng, F. H., Tie, X. X., Xu, T., Li, P., Guang, Q. Z., Qiong, Y., Xu, J. M., and Guenther, A.: Ozone photochemical production in urban Shanghai, China: analysis based on ground level observations, J. Geophys. Res., 114, doi:10.1029/2008JD010752, 2009.
Shao, M., Zhang, Y. H., Zeng, L. M., Tang, X. Y., Zhang, J., Zhong, L. J., and Wang, B. G.: Ground-level ozone in the Pearl River Delta and the roles of VOC and NO_x in its production, Environ. Manage., 90, 512–518, 2009.
Sillman, S.: The use of NO_y, H_2O_2, and HNO_3 as indicators for ozone-NO_x-hydrocarbon sensitivity in urban locations, J. Geophys. Res., 100, 14175–14188, 1995.
Sillman, S.: The relation between ozone, NO_x and hydrocarbons in urban and polluted rural environment, Atmos. Environ., 33, 1821–1845, 1999.
Tie, X., Madronich, S., Li, G. H., Ying, Z. M., Zhang, R. Y., Garcia, A. R., Taylor, J. L., and Liu, Y. B.: Characterizations of chemical oxidants in Mexico City: a regional chemical/dynamical model (WRF-Chem) study, Atmos. Environ., 41, 1989–2008, 2007.
Wang, B. G., Zhang, Y. H., and Shao, M.: Special and temporal distribution character of VOCs in the ambient air of Pearl River Delta region, Environ. Sci., 25, 7–15, 2004.
Wang, T., Wei, X. L., Ding, A. J., Poon, C. N., Lam, K. S., Li, Y. S., Chan, L. Y., and Anson, M.: Increasing surface ozone concentrations in the background atmosphere of Southern China, 1994–2007, Atmos. Chem. Phys., 9, 6217–6227, doi:10.5194/acp-9-6217-2009, 2009.
Wang, T. J., Jiang, F., Deng, J. J., Shen, Y., Fu, Q. Y., Wang, Q., Fu, Y., Xu, J. H., and Zhang, D. N.: Urban air quality and regional haze weather forecast for Yangtze River Delta region, Atmos. Environ., 58, 70–83, 2012.
Wang, X. M., Carmichael, G., Chen, D. L., Tang, Y. H., and Wang, T. J.: Impacts of different emission sources on air quality during March 2001 in the Pearl River Delta (PRD) region, Atmos. Environ., 39, 5227–5241, 2005.

ACPD
14, 18849–18877, 2014

Zhang, R. Y., Lei, W. F., Tie, X. X., and Hess, P.: Industrial emissions cause extreme diurnal urban ozone variability, P. Natl. Acad. Sci. USA, 101, 6346–6350, 2004.
Zhang, Y. H., Su, H., Zhong, L. J., Cheng, Y. F., Zeng, L. M., Wang, X. S., Xiang, Y. R., Wang, J. L., Gao, D. F., and Shao, M.: Regional ozone pollution and observation-based approach for analyzing ozone–precursor relationship during the PRIDE-PRD2004 campaign, Atmos. Environ., 42, 6203–6218, doi:10.1016/j.atmosenv.2008.05.002, 2008.
Zhao, P. S., Zhang, X. L., Xu, X. F., and Zhao X. J.: Long-term visibility trends and characteristics in the region of Bejing, Tianjin, and Hebei, China, Atmos. Res., 101, 711–718, 2011.
Zou, Y., Deng, X. J., Wang, B. G., Li, F., and Huang, Q.: Pollution characteristics of volatile organic compounds in Panyu Composition Station, Environ. Sci., 33, 808–813, 2013.

ACPD
14, 18849–18877, 2014

Table 1. The wind speed and temperature in four seasons (from June 2011 to May 2012) at GPACS.

		Minimum	Maximum	Mean value	Median
Spring	Wind speed/ms^{-1}	0	5.4	1.3	1.2
	Temperature/°C	9.4	35.5	22.6	22.9
Summer	Wind speed/ms^{-1}	0	6.0	1.4	1.2
	Temperature/°C	23.9	37.1	29.4	28.8
Autumn	Wind speed/ms^{-1}	0	5.7	1.5	1.4
	Temperature/°C	16.2	35.3	25.2	25.2
Winter	Wind speed/ms^{-1}	0	6.3	1.5	1.4
	Temperature/°C	4.7	26.9	14.2	14.1

ACPD
14, 18849–18877, 2014

Table 2. Photochemical properties of VOCs and their average mixing ratios at GPACS from Jun 2011 to May 2012.

Compound	MIR[a]	$K^{b}_{OH} \times 10^{12}$	Mixing ratio (ppbv)	Mixing ratio (ppbc)
Alkanes				
Ethane	0.25	0.27	3.66	7.31
Propane	0.46	1.15	4.34	13.02
i-Butane	1.18	2.34	2.67	10.68
n-Butane	1.08	2.54	3.07	12.28
Cyclopentane	2.24	5.16	0.15	0.77
i-Pentane	1.36	3.9	1.72	8.61
n-Pentane	1.22	3.94	1.37	6.86
Methylcyclopentane	1.46	5.1	0.32	1.94
2,3-Dimethylbutane	1.07	6.3	0.13	0.76
2-Methylpentane	1.4	5.6	0.88	5.29
3-Methylpentane	1.69	5.7	0.75	4.51
n-Hexane	1.14	5.6	1.43	8.56
2,4-Dimethylpentane	1.11	5.7	0.37	0.41
Cyclohexane	1.14	7.49	1.65	9.90
2-Methylhexane	1.09	6.9	0.58	4.04
2,3-Dimethylpentane	1.25	5.1	0.26	1.82
3-Methylhexane	1.5	5.1	0.52	3.66
2,2,4-Trimethylpentane	1.2	3.68	0.22	1.79
n-Heptane	0.97	7.15	0.32	2.24
Methylcyclohexane	1.56	10.4	0.26	1.81
2,3,4-Trimethylpentane	0.97	7	0.12	0.96
2-Methylheptane	1.12	8.3	0.08	0.66
3-Methylheptane	0.8	8.6	0.08	0.68
n-Octane	0.68	8.68	0.19	1.54
n-Nonane	0.59	10.2	0.35	3.18
n-Decane	0.52	11.6	0.03	0.29
n-Undecane	0.47	13.2	0.17	1.92
n-Dodecane	0.38	14.2	0.14	1.65

MIR[a] denotes maximum incremental reactivity (Carter et al., 1994)
k^{b}_{OH} denotes rate constant of VOCs react with hydroxyl radicals at 298 K (Atkinson and Arey, 2003)

ACPD
14, 18849–18877, 2014

Table 2. Continued.

Compound	MIR[a]	$K^{b}_{OH} \times 10^{12}$	Mixing ratio (ppbv)	Mixing ratio (ppbc)
Alkenes				
Ethene	7.4	8.5	2.99	5.97
Propene	11.57	26.3	1.32	3.96
trans-2-Butene	15.2	64	0.28	1.14
1-Butene	9.57	31.4	0.44	1.77
cis-2-Butene	14.26	56.4	0.22	0.86
trans-2-Pentene	10.47	67	0.03	0.15
1-Pentene	7.07	31.4	0.05	0.23
cis-2-Pentene	10.28	65	0.19	0.97
Isoprene	10.48	101	1.14	5.72
1-Hexene	–	–	0.67	3.99
Aromatics				
Toluene	3.93	5.96	4.59	32.10
Ethylbenzene	2.96	6.96	1.48	11.81
m,p-Xylene	8.54	20.5	1.41	11.24
Styrene	1.66	58	0.41	3.25
o-Xylene	7.58	13.6	0.66	5.28
i-Propylbenzene	2.45	6.6	0.10	0.86
n-Propylbenzene	1.96	5.7	0.23	2.05
m-Ethyltoluene	7.39	18.6	0.25	2.22
p-Ethyltoluene	4.39	11.8	0.21	1.89
1,3,5-Trimethylbenzene	11.75	56.7	0.21	1.86
o-Ethyltoluene	5.54	11.9	0.27	2.47
1,2,4-Trimethylbenzene	8.83	32.5	0.21	1.92
1,2,3-Trimethylbenzene	11.94	32.7	0.15	1.32
m-Diethylbenzene	7.08	15	0.12	1.25
p-Diethylbenzen	4.39	10	0.11	1.05

MIR[a] denotes maximum incremental reactivity (Carter et al., 1994)
k^{b}_{OH} denotes rate constant of VOCs react with hydroxyl radicals at 298 K (Atkinson and Arey, 2003)

ACPD
14, 18849–18877, 2014

Table 3. Top 10 VOCs species at GPACS based on the Propy-Equiv and MIR scales from Jun 2011 to May 2012.

OH Reactivity Rank		MIR Rank	
Compound	Percentage (%)	Compound	Percentage (%)
Isoprene	19.97	Toluene	16.26
m,p-Xylene	7.97	m,p-Xylene	12.48
Toluene	6.62	Isoprene	7.99
Styrene	6.51	Propene	6.30
1,3,5-Trimethylbenzene	3.82	Ethene	6.07
Propene	3.60	o-Xylene	5.21
Ethylbenzene	2.85	Ethylbenzene	4.54
Cyclohexane	2.56	1,3,5-Trimethylbenzene	2.87
trans-2-Butene	2.51	trans-2-Butene	2.37
o-Xylene	2.48	1,2,4-Trimethylbenzene	2.22

ACPD
14, 18849–18877, 2014

Figure 1. Location of observation site at GPACS and its surrounding area (from Google Maps).

ACPD
14, 18849–18877, 2014

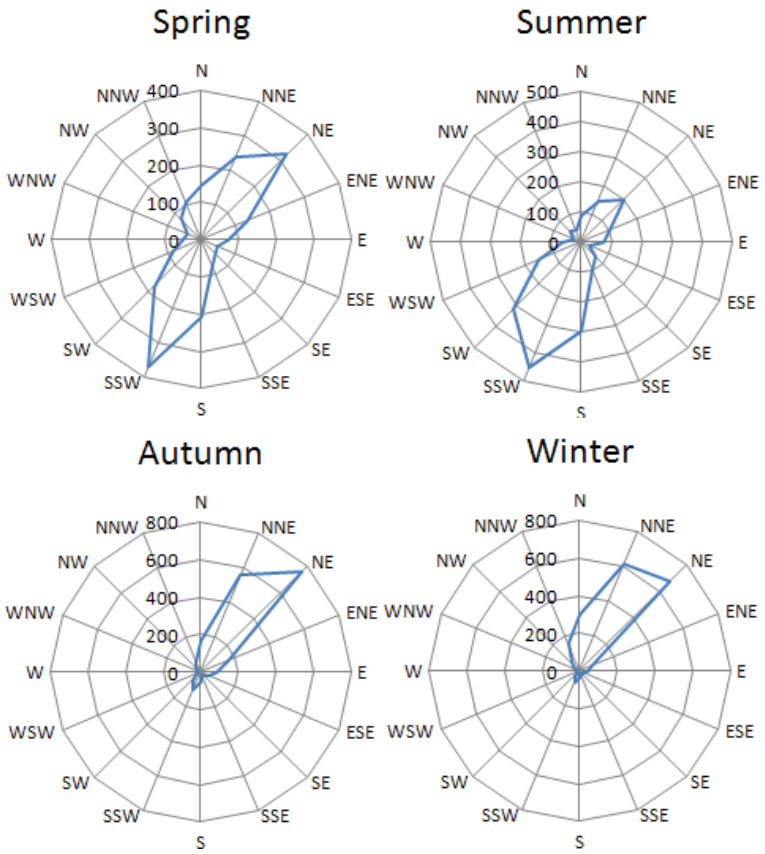

Figure 2. The frequency of wind direction plotted by wind rose for four seasons (from June 2011 to May 2012) at GPACS

ACPD
14, 18849–18877, 2014

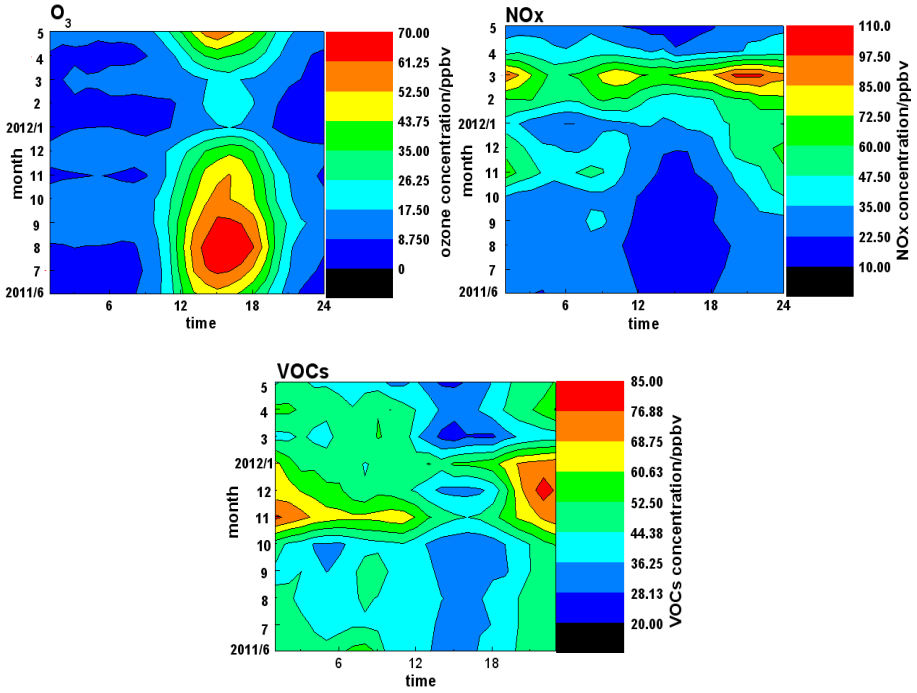

Figure 3. The diurnal variations of ozone, NO_x and VOCs in months (from June 2011 to May 2012) at GPACS.

ACPD
14, 18849–18877, 2014

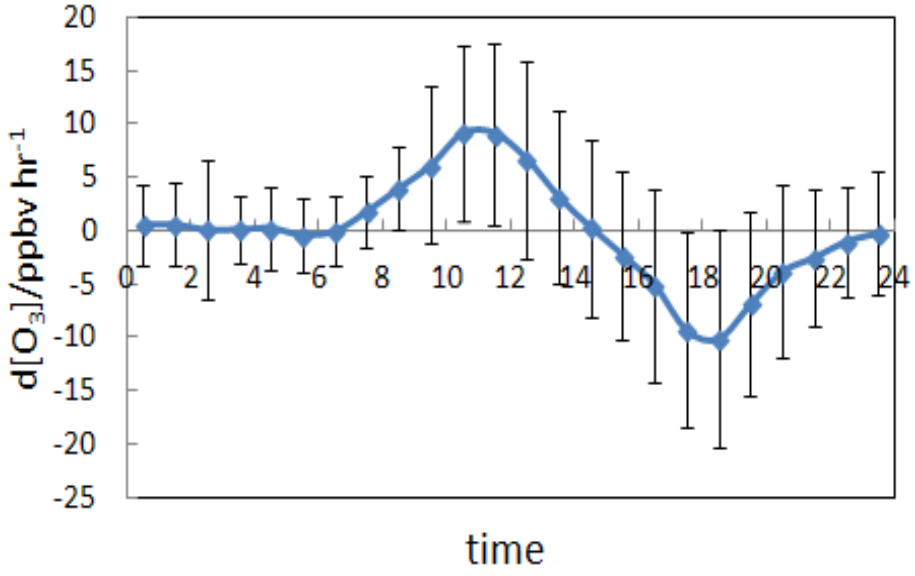

Figure 4. Average diurnal trends in ozone from June 2011 to May 2012 at GPACS. Colored marker represents hourly mean value. The black line gives the standard deviation.

ACPD
14, 18849–18877, 2014

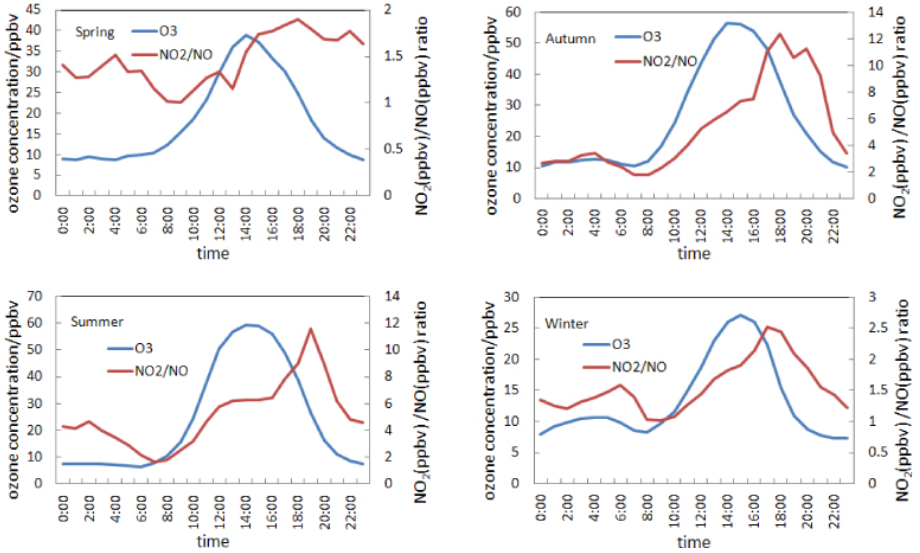

Figure 5. The relationship between NO_2/NO ratio and ozone in four seasons (from June 2011 to May 2012) at GPACS. Colored markers represent hourly mean values.

ACPD
14, 18849–18877, 2014

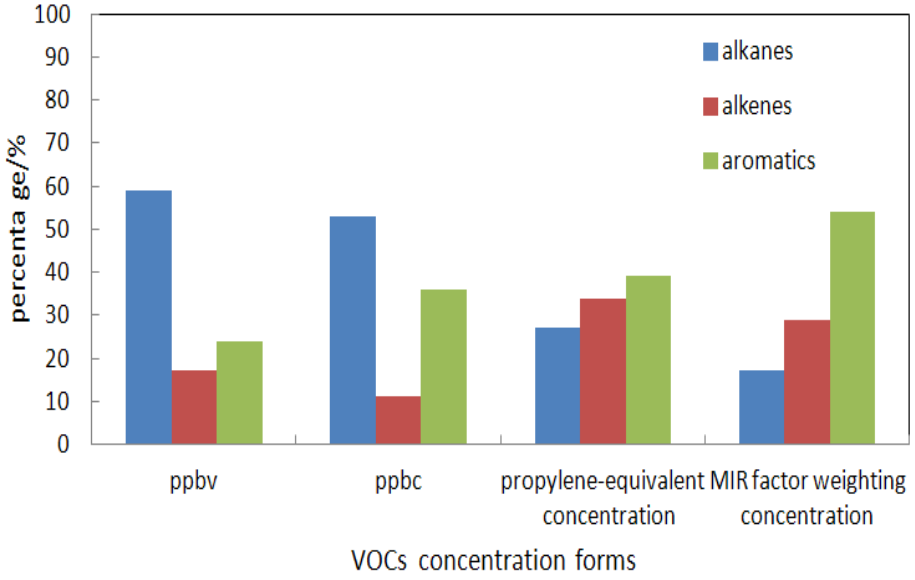

Figure 6. Average fractions of each category based on volume mixing ratio (ppbv), carbon-atom-based concentration (ppbC), OH-reactivity-based Propy-Equiv concentration (ppbC), and MIR factor weighting concentration. Fractions of each VOCs category (alkanes, alkenes and aromatics) plotted by bar on four VOCs concentration form (ppbv, ppbc, propylene-equivalent concentration and MIR factor weighting concentration) from June 2011 to May 2012 at GPACS.

ACPD
14, 18849–18877, 2014

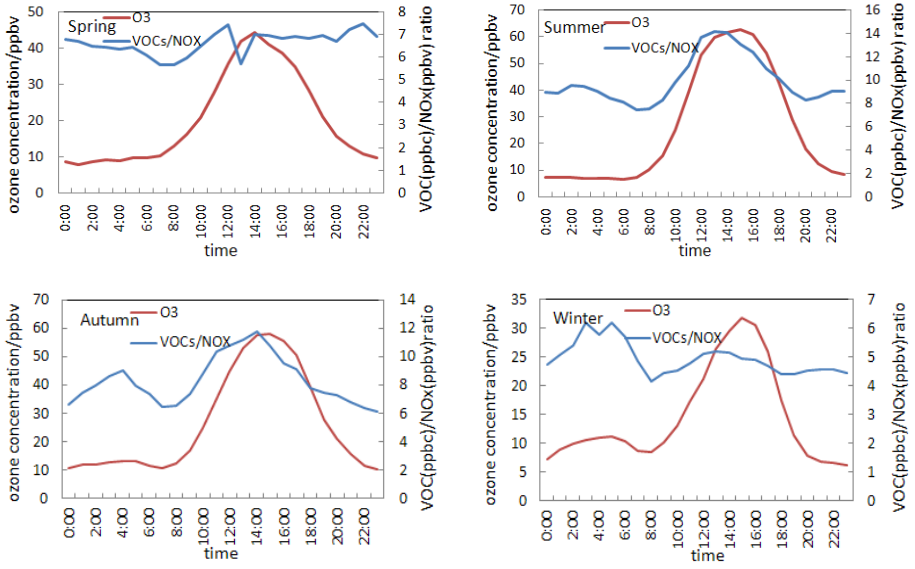

Figure 7. The variation patterns of VOC/NO_x ratio and ozone concentration at four seasons (from June 2011 to May 2012) at GPACS. Colored markers represent hourly mean value.

ACPD
14, 18849–18877, 2014

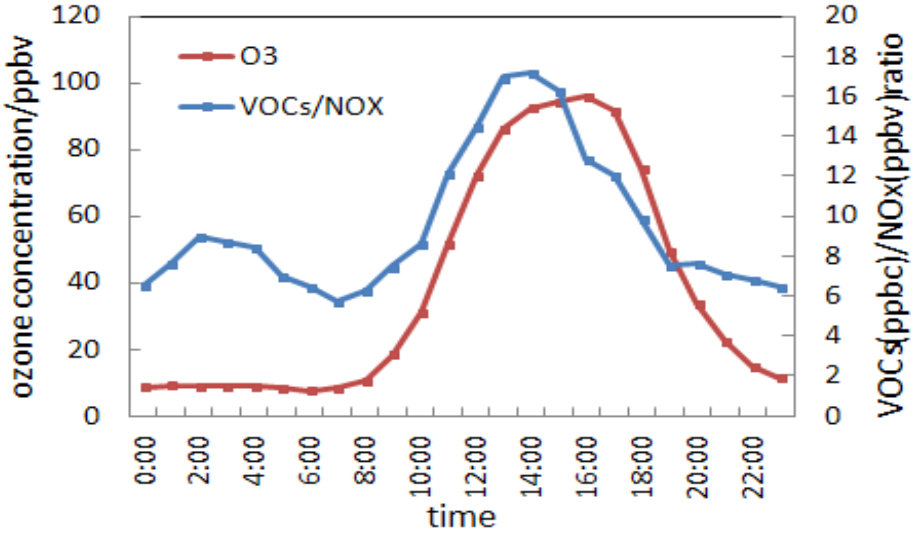

Figure 8. The variation patterns of VOC/NO_x ratio and ozone concentration at high ozone episode at GPACS. Colored markers represent hourly mean value. High ozone episode refers to the day with an hourly ozone value higher than 93 ppbv.

ACPD
14, 18849–18877, 2014